

# The polyacrylic latex: an efficient water-soluble binder for $\text{LiNi}_{1/3}\text{Co}_{1/3}\text{Mn}_{1/3}\text{O}_2$ cathode in li-ion batteries

Haoxiang Zhong<sup>1</sup> · Minghao Sun<sup>1,2</sup> · Yong Li<sup>1,2</sup> · Jiarong He<sup>1,2</sup> · Jianwen Yang<sup>3</sup> · Lingzhi Zhang<sup>1</sup>

Received: 19 March 2015 / Revised: 2 May 2015 / Accepted: 12 July 2015 / Published online: 1 August 2015  
© Springer-Verlag Berlin Heidelberg 2015

**Abstract** The polyacrylic latex (LA132) was firstly reported as a water-soluble binder for  $\text{LiNi}_{1/3}\text{Co}_{1/3}\text{Mn}_{1/3}\text{O}_2$  (NCM) cathode in Li-ion battery. The electrochemical performances of NCM cathode with LA132 binder were investigated and compared with the conventional water-soluble sodium carboxymethyl cellulose (CMC) and commercial non-aqueous polyvinylidene difluoride (PVDF). NCM cathode with LA132 binder exhibited a much higher specific capacity of  $146 \text{ mAh g}^{-1}$  and capacity retention of 96.4 % after 100 cycles as compared with  $122 \text{ mAh g}^{-1}/88 \%$  and  $121 \text{ mAh g}^{-1}/75\%$  for the NCM electrode with CMC and PVDF, respectively. In addition, NCM cathode with LA132 binder exhibited better rate capability than that of CMC and PVDF, e.g., retaining 34.3 % capacity of C/5 at 5 C rate as compared with 28.5 and 10.9 % for CMC and PVDF, respectively.

**Keywords** Water-soluble binder · Cathode ·  $\text{LiNi}_{1/3}\text{Co}_{1/3}\text{Mn}_{1/3}\text{O}_2$  · Li-ion battery

## Introduction

Although the binders are electrochemically inactive materials, they can have a significant influence on the electrochemical

performances of Li-ion batteries (LIBs) [3, 14]. Currently, poly(vinylidene difluoride) (PVDF) has been widely used as the binder for both the negative and positive electrodes in commercial LIBs because of its good stability and high adhesion to electrode materials and current collectors [10]. However, there still remain some drawbacks for PVDF used as a binder in Li-ion batteries. Generally, PVDF has to be dissolved in a volatile, toxic N-methyl-2-pyrrolidone (NMP), which poses serious pollution to the environment. Furthermore, low flexibility, high cost, and poor recyclability are unfavorable to its application in large-scale batteries [9]. Thus, much effort has been devoted recently to developing a cheap, environment-friendly water soluble binder to replace the PVDF/NMP binder system [25].

Water soluble polymers, such as carboxymethyl cellulose (CMC) [20, 35], polyacrylate (PAA) [6], and alginate [1, 8, 31] have been explored as binders for use in Li-ion battery. However, these works primarily focused on their applications for anode materials such as graphite, silicon, or  $\text{Li}_4\text{Ti}_5\text{O}_{12}$ . Recently, remarkable research has been reported on exploring these water soluble binders for cathode materials. Carboxymethyl cellulose (CMC) [24, 35], polyacrylic acid (PAA) [2, 30], and polyacrylic latex (LA132) [11, 12] have already been used as binders for cathode materials, such as lithium iron phosphate (LFP), lithium cobalt oxide (LCO), and lithium manganese oxide (LMO). These water soluble polymers have some advantages over the commercial non-aqueous PVDF in improving electrochemical performances of the cathode, especially the rate capability.

The layered transition-metal oxide  $\text{LiNi}_{1/3}\text{Co}_{1/3}\text{Mn}_{1/3}\text{O}_2$  is a promising cathode material due to its higher reversible capacity with milder thermal stability, lower cost, and less toxicity than  $\text{LiCoO}_2$  [15, 34], while relatively fewer water soluble binders were used for  $\text{LiNi}_{1/3}\text{Co}_{1/3}\text{Mn}_{1/3}\text{O}_2$  (NCM) electrode due to its stronger basicity. Recently, it has been reported

✉ Lingzhi Zhang  
lzzhang@ms.giec.ac.cn

<sup>1</sup> Key Laboratory of Renewable Energy, Guangzhou Institute of Energy Conversion, Chinese Academy of Sciences, Guangzhou, Guangdong 510640, China

<sup>2</sup> University of Chinese Academy of Sciences, Beijing 100039, China

<sup>3</sup> College of Chemistry & Bioengineering, Guilin University of Technology, Jiangan Road, Guilin, Guangxi 541004, China

that NCM electrode with CMC binder exhibited better electrochemical properties than that of PVDF and alginate [4, 5, 26, 27]. However, the electrode slurry using CMC binder has difficult to be dispersed homogeneously onto an Al foil during fabricating of the electrode sheet. Moreover, CMC is also prone to bacterial growth which limits the shelf life [22].

The polyacrylic latex (LA132) is a triblock-copolymer of acrylamide (AM), lithium methacrylate (LiMAA), and acrylonitrile (AN), which shows good stability and high adhesion property. Recently, LA132 has been reported as the binder for electrode materials, such as LFP and LCO [11, 12], and demonstrated promising electrochemical performances. So far, it has not yet been used as a binder for NCM cathode. In this work, we report our investigation on LA132 as a binder for NCM cathode, and compare its electrochemical performances with the conventional water soluble binders of CMC and the commercial non-aqueous PVDF binder.

## Experimental

NCM powder was obtained from Advanced Electronics Energy Co. (China). The polyacrylic latex (LA132, Indigo, China) was used in the form of an aqueous emulsion of 15 wt% with a viscosity of 5000–6000 mPa·s at 40 °C. PVDF (Solvay Solef®5130) was donated by Shenzhen Micro Electron Co. (China). CMC (viscosity=800–1200 mPa·s) was purchased from Aladdin Chemistry Co. (China). The electrolyte of 1 M LiPF<sub>6</sub> in ethylene carbonate (EC, ≥99.9 %)/diethylene carbonate (DEC, ≥99.9 %)/dimethyl carbonate (DMC, ≥99.9 %) (1/1/1, by volume) was purchased from Zhangjiagang Guotai-Huarong New Chemical Materials Co. (China) (water content <10 ppm).

NCM powder was mixed with carbon black and LA132 binder in a weight ratio of 90:5:1 in an aqueous solution to form homogeneous slurry. For comparisons, common proportion of PVDF-based electrode with 90 wt% NCM, 5 wt% carbon black, 5 wt% PVDF and a CMC-based electrode with 90 wt% NCM, 5 wt% carbon black, and 5 wt.% CMC were used, respectively. The slurry was coated onto a 20- $\mu$ m-thick aluminum foil. The obtained electrodes were dried at 70 °C for 3 h and then dried at 90 °C in a vacuum oven for 12 h to remove the solvent thoroughly. In addition, the different amounts of LA132 binder have been conducted during fabricating NCM electrode sheets. NCM powder was mixed with carbon black and LA132 in a weight ratio of 90:5:0.5, 90:5:1, 90:5:1.5, and 90:5:5, respectively. For the sake of convenience, the used LA132 above was expressed in LA (1), LA (2), LA (3), and LA (4), respectively. The cell (2032) was assembled to test the electrochemical performances after the moisture of NCM electrodes was measured. Circular electrodes were punched out with an area of 1.76 cm<sup>2</sup> and a loading level of 6.25 mg cm<sup>-2</sup>. Pure lithium metal was used as the counter and reference electrode. The cells were

galvanostatically charged and discharged in a voltage range of 2.8–4.3 V at room temperature (25 °C).

The phase identification of the active material was performed by X-ray diffraction (XRD, PANALYTICAL Incorporated, Netherlands) from 10 to 80°. The morphologies of NCM electrodes were observed by scanning electron microscope (SEM; Hitachi S-4800, Japan) equipped with an energy-dispersive spectroscopy detector (EDS). The moisture of the electrode sheet was measured by Metrohm's 899 KF coulometer equipped with Metrohm's 860 KF oven. Cyclic voltammetry (CV) was measured on with a Zennium/IM6 electrochemical workstation (Zahner, Germany) between 2.8 and 4.3 V (vs. Li/Li<sup>+</sup>) at a scanning rate of 0.2 mV·s<sup>-1</sup>. Electrochemical impedance spectroscopy (EIS) measurements were also measured at the electrochemical workstation after different cycles by applying an alternating voltage of 5 mV over the frequency ranging from 10<sup>-2</sup> to 10<sup>5</sup> Hz. Adhesion strength of the polymer layers onto the Al current collectors were tested using a 180° peel tester from Shenzhen Kaiqiagli testing instruments Co. (China).

## Results and discussion

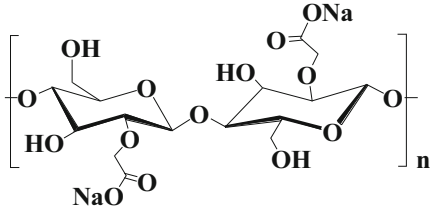
### Structure and property of LA132 binder

The structure of LA132, CMC, and PVDF polymers is illustrated in Table 1. LA132 binder is a copolymer of acrylamide (AM), lithium methacrylate (LiMAA), acrylonitrile (AN), containing high-polarity hydrophilic cyano/amide groups which supply enough adhesion strength between active material, conductive agent and current collector, and relative low-polarity oleophylic ester group which provides proper flexibility for the electrode. However, it is only high-polarity functional groups for CMC/PVDF polymers.

Linear sweep voltammetry (LSV) from open circuit voltage to 6.5 V (vs. Li/Li<sup>+</sup>) was performed on bare Al foils and Al foils coated by LA132, CMC, or PVDF, respectively. An electrochemical cell consisting of Al foil (working electrode) and lithium metal (counter electrode) was used to determine the oxidation stability of LA132 and compared with CMC and PVDF. The limiting oxidation stability of the binder is shown in Fig. 1. LA132, CMC, or PVDF did not show any current peaks up to 4.4 V, indicative of good oxidation stability. Therefore, LA132 can be used as the binder for NCM electrode from 2.8 to 4.3 V.

Adhesion strength of the binder onto the Al current collector was measured by the peel test experiment with the same method [28], and the results are summarized in Table 2. LA (2) binder shows higher adhesion strength (0.54 N cm<sup>-1</sup>) than that of CMC (0.04 N cm<sup>-1</sup>) and PVDF (0.36 N cm<sup>-1</sup>). The higher adhesion strength of LA binder is closely relative to its unique structure with high-polarity cyano and amide groups.

**Table 1** Molecular structures of LA, CMC, and PVDF

Binder	Structure
LA	$\left[ \text{CH}_2 - \underset{\text{H}}{\overset{\text{R}_1}{\text{C}}} - \text{CH}_2 - \underset{\text{CH}_3}{\overset{\text{R}_2}{\text{C}}} - \text{H}_2\text{C} - \underset{\text{H}}{\overset{\text{R}_3}{\text{C}}} \right]_n$ <p>(R<sub>1</sub> -Acrylamide, R<sub>2</sub> -Carboxylic acid lithium, R<sub>3</sub> Cyano-)</p>
CMC	
PVDF	$\left[ \begin{array}{cc} \text{H} & \text{F} \\   &   \\ -\text{C} & - & \text{C}- \\   &   \\ \text{H} & \text{F} \end{array} \right]_n$

Due to higher adhesion property, LA (2) binder with the lower content was used during fabricating NCM electrode sheets, as compared with CMC and PVDF, respectively (Table 3).

**Structure and morphology of LiNi<sub>1/3</sub>Mn<sub>1/3</sub>Co<sub>1/3</sub>O<sub>2</sub>**

NCM sample has been characterized by X-ray diffraction. As seen in Fig. 2a, the Bragg lines are well indexed in the R-3m

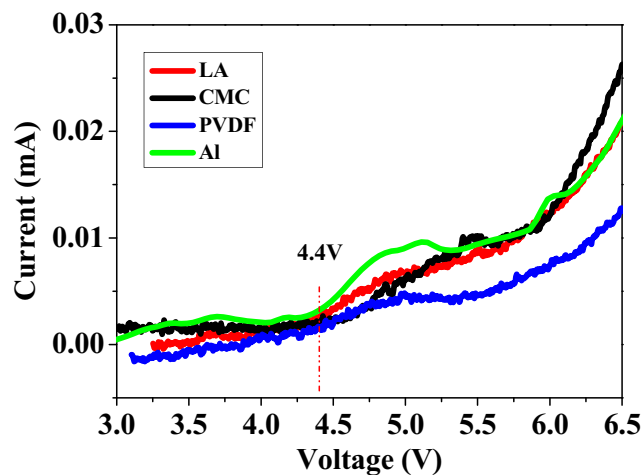


**Fig. 1** Oxidation stability of LA132 compared to PVDF/CMC

space group with the hexagonal ordering. No impurity phases are detected, and the powders are well crystallized in the α-NaFeO<sub>2</sub> type structure [21, 23]. The good distribution of active material, carbon black, and the binder in the electrode sheet would be beneficial to the electrochemical properties [13, 33]. To investigate this issue, photographs of NCM electrodes sheets with LA (2), CMC, and PVDF binders were shown in Fig. 2b–d. For LA and PVDF binders, the NCM electrode exhibited a smooth and uniform surface (inset of Fig. 2b, 2c), while relatively coarse surface appeared for NCM electrode with CMC binder (inset of Fig. 2d). SEM images of NCM electrodes with different binders are further observed in Fig. 2b–d. NCM electrodes with LA or PVDF binder are dispersed homogeneously and kept perfectly (Fig. 2b–c). While for CMC system, lots of cracks were observed (Fig. 2d).

**Table 2** Adhesion strength of the binders to the Al current collector

Binder	Peel force (N)	Peel strength (N cm <sup>-1</sup> )
LA	0.811	0.54
CMC	0.058	0.04
PVDF	0.539	0.36

**Table 3** Electronic conductivity of NCM electrodes plates with different binders

Binder	Conductivity(S/cm)
NCM/AB/LA	0.084
NCM/AB/CMC	0.068
NCM/AB/PVDF	0.13

The corrosion of the aluminum substrate has been reported, and the rate of aluminum corrosion increased with higher temperature and longer time during the water processing of NCM slurry [5, 7].

In order to make clear whether the corrosion of the aluminum foil could occur in our experiment condition, we performed SEM studies on the aluminum foil-coated layer of NCM electrodes and fresh aluminum foil. The fresh foil exhibits coarse surface with very few pits (Fig. 3a). NCM electrode coatings on aluminum foil were removed prior to SEM characterization. There are no distinct differences between Al foil-coated NCM slurry with LA binder and the fresh aluminum, while quite a few pits are observed in the Al foil-coated NCM electrode with CMC binder (Fig. 3b/c), which indicated that the Al foil corrosion in NCM electrode with LA binder could not appear but for CMC binder.

### Electrochemical performances

The cycling performance of NCM electrodes (the moisture of NCM electrodes <300 ppm) with different contents of LA (1–4)

binder was shown in Fig. 4a. At C/5 rate, NCM electrode delivers specific capacity of 136, 146, 140, and 127 mAh g<sup>-1</sup> with capacity retention of 94.9, 96.2, 94.2, and 86.7 % after 100 cycles with LA (1–4), respectively. NCM electrode with LA (2) shows the highest specific capacity and best capacity retention than that of LA (1, 3, 4). For LA/AB (1:1, by mass) in NCM electrode (NCM/AB/binder=90:5:5), LA binder helps to form a conducting network of AB in NCM electrode sheet, but excessive LA aggregates in a separate insulating phase. Electrons can pass through the conducting network but not the polymer phase [17–19]. As a result, NCM electrode with LA (4) (LA/AB=1:1) shows inferior cycle performance than that of LA (1–3), probably due to the excess insulating LA in the electrode composition. When decreasing the LA ratio to (LA/AB=1:5), LA still exhibits a satisfied adhesion capability for AB/NCM. Therefore, NCM electrode with the optimized ratio of LA (2) (NCM/AB/LA=90:5:1) showed better cycle performance than that of LA (1,3, 4). The three electrodes at C/5 rate after 100 cycles deliver specific capacity of 146, 122, and 121 mAh g<sup>-1</sup> with capacity retention of 96.2, 88, and 75 % for NCM electrodes with LA (2), CMC, and PVDF, respectively. Extending 200 cycles, NCM electrode with LA (2) exhibits a specific capacity of 140 mAh g<sup>-1</sup> with 92 % capacity retention, demonstrating better cycling stability than that of CMC and PVDF (Fig. 4b). Figure 4c showed the rate capability of NCM electrodes with LA (2), CMC, and PVDF, respectively. The rate was increased gradually from C/5 to 5 C and finally returned to C/5. At rates from C/10 to 1 C, NCM electrodes with LA (2) exhibited a similar rate performance with that of PVDF, but far higher than

**Fig. 2** **a** XRD pattern of NCM sample. **b–d** SEM images of NCM electrodes prepared with different binders **b** LA (2), **c** PVDF, and **d** CMC. *Inset* represents photographs of the single electrode sheets

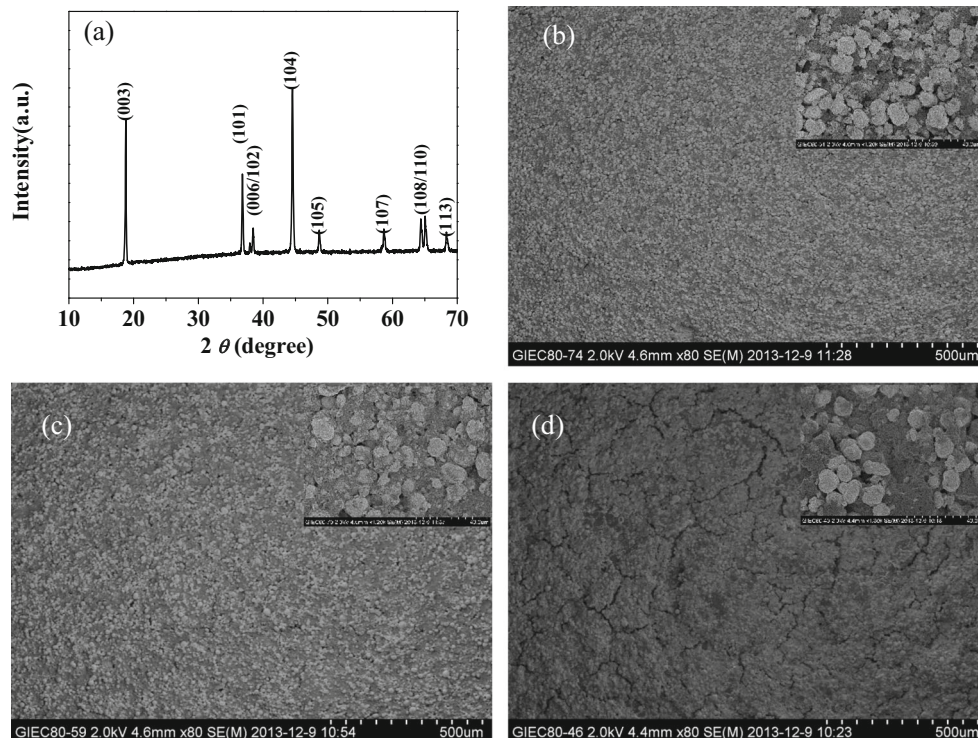
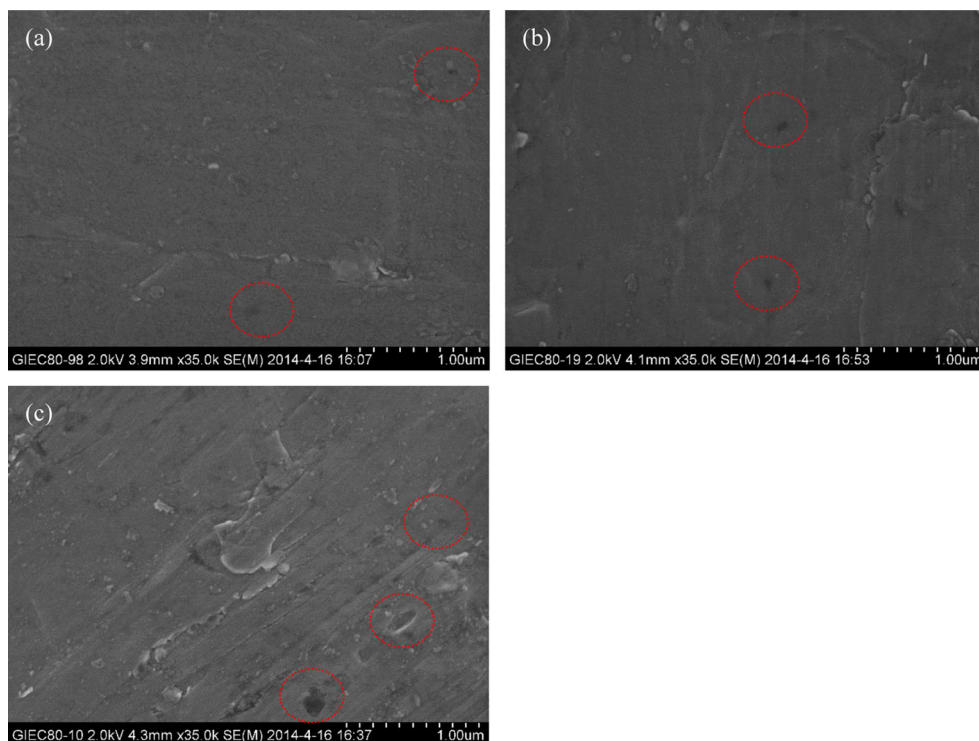




**Fig. 3** SEM images of **a** fresh Al. **b–c** Al foil surface after removal of the coatings prepared electrodes with different binders **b** LA (2), and **c** CMC



that of CMC. At higher than 2 C rate, NCM electrodes with LA (2) exhibited better rate capability than CMC or PVDF. For example, at 5 C rate, NCM electrodes with LA (2) delivered

specific capacity and capacity retention of 52 mAh g<sup>-1</sup>/34.3 %, while only 37 mAh g<sup>-1</sup>/28.5 % and 18 mAh g<sup>-1</sup>/10.9 % for CMC and PVDF, respectively. When the high-rate tests were

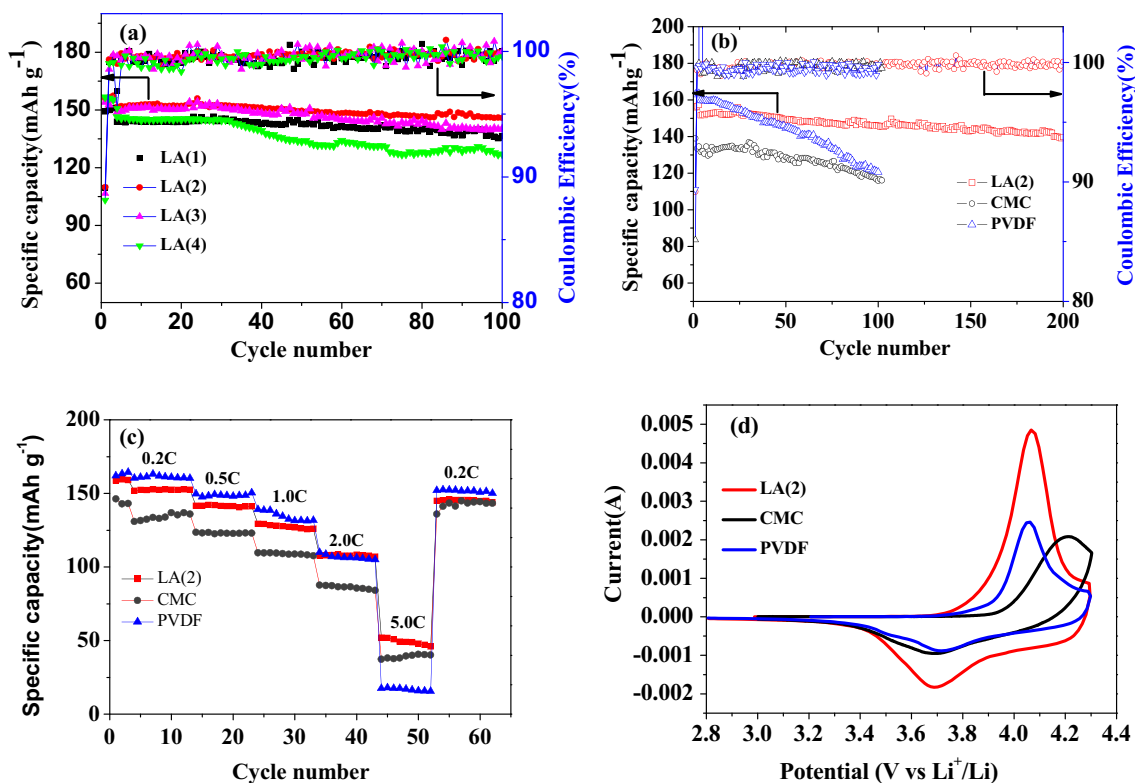
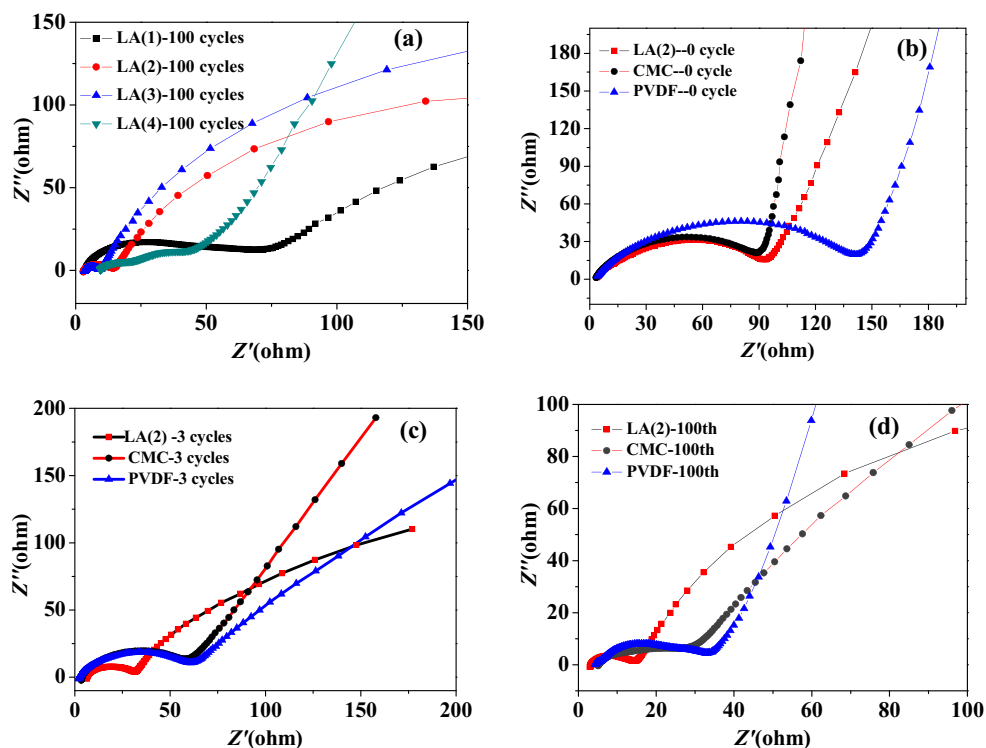


**Fig. 4** The cycling performance of NCM electrode (**a–b**), **a** different amounts of LA and **b** different binders, **c** the rate capability of NCM electrodes with different binders, and **d** CV of NCM electrodes with different binders

**Fig. 5** Nyquist plots of NCM electrodes with different binders by applying an alternating voltage of 5 mV over the frequency ranging from  $10^{-2}$  to  $10^5$  Hz. **a** different amounts of LA 132 after 100 cycles, **b–d** NCM electrodes with different binders after different cycles, **b** 0 cycle, **c** 3 cycles, and **d** 100 cycles

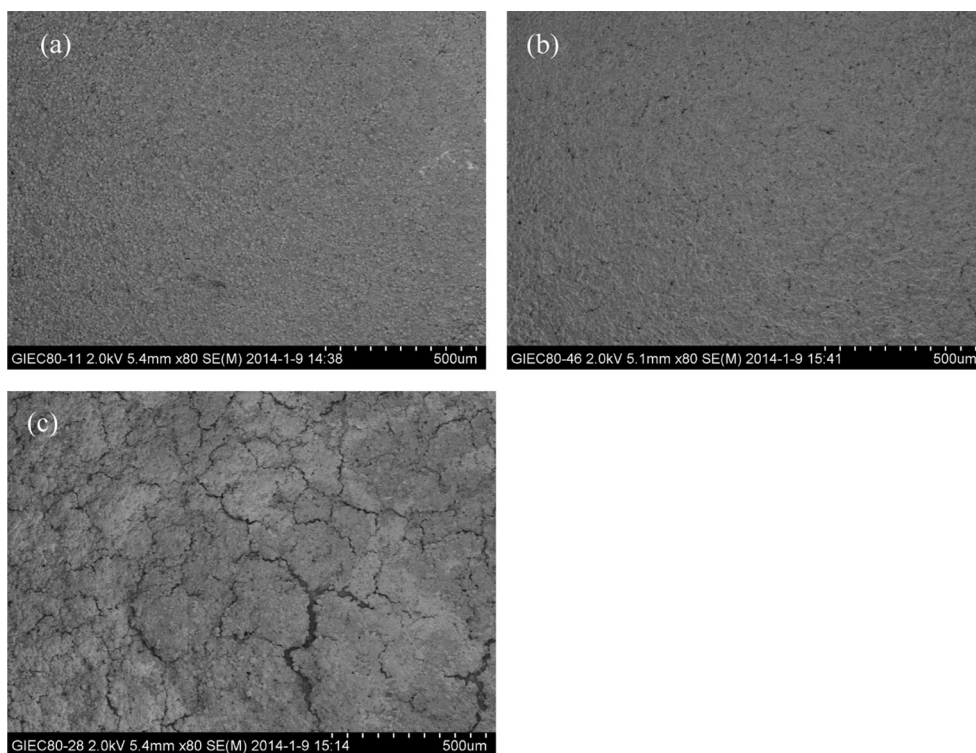


completed and changed back to C/5, the specific capacity of the three electrodes remained the same as before, which was confirmed that all of them performed well. In spite of the lower content binder used, the NCM electrode with LA (2) showed better electrochemical properties than PVDF/CMC,

further exhibiting the advantages of LA binder for NCM electrodes.

CV was performed on NCM electrodes with three different binders at a scan rate of  $0.2 \text{ mV s}^{-1}$  from 2.8 to 4.3 V in Fig. 4d. The oxidation and reduction peaks of NCM with the

**Fig. 6** a–c SEM images of NCM electrodes with different binders after 100 cycles, **a** LA (2), **b** PVDF, and **c** CMC



three binders appeared at around 4.1 and 3.7 V, which was typically observed for NCM cathodes [29]. The separation between redox peaks was 0.37, 0.5, and 0.35 V for NCM with LA (2), CMC, and PVDF, respectively. NCM with LA (2) showed comparable separation between redox peaks with that of PVDF, but much smaller than that of CMC, thus lower concentration polarization than that of CMC.

Figure 5 displayed the Nyquist plots of NCM electrodes with LA, PVDF, and CMC over different cycles. All Nyquist plots consisted of a depressed semicircle in the high-frequency region, the semicircle at medium frequency range correlated with the electron transfer resistance ( $R_{ct}$ ), and the straight line at lower frequency corresponding to  $\text{Li}^+$  diffusion resistance in electrode bulk, namely the Warburg impedance [16, 32]. Figure 5a compared the Nyquist plots of NCM electrodes with different contents of LA (1–4) binder over 100 cycles. The intercept with the real axis ( $Z'$ ) at the high frequency indicated that NCM electrodes with LA (1–3) have the lower ohmic resistance than LA (4). Moreover, the diameter of the semicircle reflecting the interfacial resistance was in order of LA (2)~LA (3)<LA (1)<LA (4), which was in well accordance with the cycling performance of NCM electrodes with LA (1–4). Figure 5b–d compared the Nyquist plots of NCM electrodes over different cycles with LA (2), CMC, and PVDF, respectively. The ohmic resistance of NCM electrodes decreased with increased cycles from 0, 3 to 100. NCM electrode with LA (2) binder showed a smaller semicircle diameter at the high/middle frequency compared with CMC and PVDF, indicating an improved kinetic of electrode reactions (i.e., charge transfer and polarization). This is probably due to excellent slurry homogeneity and improved kinetic of electrode reactions which is essential to facilitate the transportation of lithium ions in the bulk.

SEM images of NCM electrodes with different binders after 100 cycles were presented in Fig. 6. NCM electrodes with LA and PVDF are well preserved; only larger cracks appeared for CMC, thus LA132 could potentially be used as water-soluble binder for NCM electrodes in lithium ion battery.

## Conclusions

We have demonstrated that LA132 could serve as a water-soluble binder for NCM electrode in LIBs for the first time. With optimized ratio (90:5:1) of NCM/carbon black/LA (2), NCM electrode exhibited better cycling performances and better rate capability than that of PVDF and CMC due to proper adhesion strength of LA binder and favorable electrochemical kinetics of the electrode. These results prove that LA132 could be used as a potential water-soluble binder for NCM electrode in Li-ion batteries.

**Acknowledgments** This work was supported by Fund for Science & Technology Innovation Team of Zhoushan (Zhejiang, China), Cooperative innovation Project of Science & Technology of Guangzhou (201423), Collaboration Project of CAS-Guangdong Province (2013B091300017), Guangzhou Municipal Project for Science & Technology (2014Y2-00219) and Special Support Program of Guangdong Province for High-Level Talents (2014TX01N014).

## References

1. Aaron C, Timothy B, Colin H, Kyle K, Buddie M, Brian K (2012) Influences of gold, binder and electrolyte on silicon nanowire performance in li-ion batteries. *J Phys Chem C* 116:18079–18086
2. Cai ZP, Liang Y, Li WS, Xing LD, Liao YH (2009) Preparation and performances of  $\text{LiFePO}_4$  cathode in aqueous solvent with polyacrylic acid as a binder. *J Power Sources* 189:547–551
3. Chen JC, Liu JY, Qi Y, Sun T, Li XD (2013) Unveiling the roles of binder in the mechanical integrity of electrodes for lithium-ion batteries. *J Electrochem Soc* 160:A1502–A1509
4. Doberdò I, Löffle N, Laszczynski N, Cericola D, Penazzi N, Bodoardoilvia S, Kim GT, Passerini S (2014) Performance of  $\text{LiNi}_{1/3}\text{Mn}_{1/3}\text{Co}_{1/3}\text{O}_2$ /graphite batteries based on aqueous binder. *J Power Sources* 248:915–922
5. Doberdò I, Löffle N, Laszczynski N, Cericola D, Penazzi N, Bodoardoilvia S, Kim GT, Passerini S (2014) Enabling aqueous binders for lithium battery cathodes—carbon coating of aluminum current collector. *J Power Sources* 248:1000–1006
6. Fergus JW (2010) Recent developments in cathode materials for lithium ion batteries. *J Power Sources* 195:939–954
7. Ishii K, Ozaki R, Kaneko K, Fukushima H, Masuda M (2007) Continuous monitoring of aluminum corrosion process in deaerated water. *Corros Sci* 49:2581–2601
8. Kovalenko I, Zdyrko B, Magasinski A, Hertzberg B, Milicev Z, Burtovyy R, Luzinov I, Yushin G (2011) A major constituent of brown algae for use in high-capacity li-ion batteries. *Science* 6052: 75–79
9. Li JL, Armstrong BL, Kiggans J, Daniel C, WoodIII DL (2012) Optimization of  $\text{LiFePO}_4$  nanoparticle suspensions with polyethyleneimine for aqueous processing. *Langmuir* 28:3783–3790
10. Li JL, Armstrong BL, Kiggans J, Daniel C, WoodIII DL (2013) Lithium ion cell performance enhancement using aqueous  $\text{LiFePO}_4$  cathode dispersions and polyethyleneimine dispersant. *J Electrochem Soc* 160:A201–A206
11. Li CC, Lee JT, Lo CY, Wu MS (2005) Effects of PAA- $\text{NH}_4$  addition on the dispersion property of aqueous  $\text{LiCoO}_2$  slurries and the cell performance of as-prepared  $\text{LiCoO}_2$  cathodes. *Electrochem Solid St* 8:A509–A512
12. Li CC, Lee JT, Peng XW (2006) Improvements of dispersion homogeneity and cell performance of aqueous-processed  $\text{LiCoO}_2$  cathodes by using dispersant of PAA- $\text{NH}_4$ . *J Electrochem Soc* 153:A809–A815
13. Li CC, Wang YW (2013) Importance of binder compositions to the dispersion and electrochemical properties of water-based  $\text{LiCoO}_2$  cathodes. *J Power Sources* 227:204–210
14. Ling M, Qiu JX, Li S, Zhao H, Liu G, Zhang SQ (2013) An environmentally benign LIB fabrication process using a low cost, water soluble and efficient binder. *J Mater Chem A* 1: 1543–11547
15. Liu XZ, Li HQ, Li D, Ishida M, Zhou HS (2013) PEDOT modified  $\text{LiNi}_{1/3}\text{Co}_{1/3}\text{Mn}_{1/3}\text{O}_2$  with enhanced electrochemical performance for lithium ion batteries. *J Power Sources* 243:374–380

16. Liu S, Xiong L, He C (2014) Long cycle life lithium ion battery with lithium nickel cobalt manganese oxide (NCM) cathode. *J Power Sources* 261:285–291
17. Liu G, Zheng H, Kim S, Deng Y, Minor AM, Song X, Battaglia VS (2008) Effects of various conductive additive and polymeric binder contents on the performance of lithium-ion composite cathode. *J Electrochem Soc* 155:A887–A892
18. Liu G, Zheng H, Simens AS, Minor AM, Song X, Battaglia VS (2007) Optimization of acetylene black conductive additive and PVDF composition for high-power rechargeable lithium-ion cells. *J Electrochem Soc* 154:A1129–A1134
19. Liu G, Zheng H, Song X, Battaglia VS (2012) Particles and polymer binder interaction: a controlling factor in lithium-ion electrode performance. *J Electrochem Soc* 159:A214–A221
20. Lux SF, Schappacher F, Balducci A, Passerini S, Winter MJ (2010) Low cost, environmentally benign binders for lithium-ion batteries. *J Electrochem Soc* 157:A320–A325
21. Manthiram A, Choi J (2006) Chemical and structural instabilities of lithium ion battery cathodes. *J Power Sources* 159:249–253
22. Pohjalainen E, Räsänen S, Jokinen M, Yliniemi K, Worsley DA, Kuusivaara J, Juurikivi J, Ekqvist R, Kallio T, Karppinen M (2013) Water soluble binder for fabrication of  $\text{Li}_4\text{Ti}_5\text{O}_{12}$  electrodes. *J Power Sources* 226:134–139
23. Ryu WH, Lim SJ, Kim WK, Kwon HS (2014) 3-D dumbbell-like  $\text{LiNi}_{1/3}\text{Mn}_{1/3}\text{Co}_{1/3}\text{O}_2$  cathode materials assembled with nanobuilding blocks for lithium-ion batteries. *J Power Sources* 257:186–191
24. Wang ZL, Dupré N, Gaillot AC, Lestriez B, Martin JF, Daniel L, Patoux S, Guyomard D (2012) CMC as a binder in  $\text{LiNi}_{0.4}\text{Mn}_{1.6}\text{O}_4$  5 V cathodes and their electrochemical performance for li-ion batteries. *Electrochimica Acta* 62:77–83
25. Wang JL, Yao ZD, Monroe CW, Yang J, Nuli Y (2013) Carbonyl- $\beta$ -Cyclodextrin as a novel binder for sulfur composite cathodes in rechargeable lithium batteries. *Adv Funct Mater* 23:1194–1201
26. Wu QL, Ha S, Prakash J, Dees WD, Lu WQ (2013) Investigations on high energy lithium-ion batteries with aqueous binder. *Electrochimica Acta* 114:1–6
27. Xu JT, Chou SL, Gu QF, Liu HK, Dou SX (2013) The effect of different binders on electrochemical properties of  $\text{LiNi}_{1/3}\text{Mn}_{1/3}\text{Co}_{1/3}\text{O}_2$  cathode material in lithium ion batteries. *J Power Sources* 225:172–178
28. Xu YH, Yin GP, Ma YL, Zuo PJ, Cheng XQ (2010) Simple annealing process for performance improvement of silicon anode based on polyvinylidene fluoride binder. *J Power Sources* 195:2069–2073
29. Zhang XY, Jiang WJ, Zhu XP, Mauger A, Lu Q, Julien CM (2011) Aging of  $\text{LiNi}_{1/3}\text{Mn}_{1/3}\text{Co}_{1/3}\text{O}_2$  cathode material upon exposure to  $\text{H}_2\text{O}$ . *J Power Sources* 196:5102–5108
30. Zhang ZA, Zeng T, Qu CM, Lu H, Jia M, Lai YQ, Li J (2012) Cycle performance improvement of  $\text{LiFePO}_4$  cathode with polyacrylic acid as binder. *Electrochimica Acta* 80:440–444
31. Zhang L, Zhang LY, Chai LL, Xue P, Hao WW, Zheng HH (2014) A coordinatively cross-linked polymeric network as a functional binder for high-performance silicon submicroparticle anodes in lithium-ion batteries. *J Mater Chem A* 2:19036–19045
32. Zheng HH, Tan L, Liu G, Song XY, Battaglia VS (2012) Calendering effects on the physical and electrochemical properties of  $\text{Li}[\text{Ni}_{1/3}\text{Mn}_{1/3}\text{Co}_{1/3}]\text{O}_2$  cathode. *J Power Sources* 208:52–57
33. Zheng HH, Yang RZ, Liu G, Song XY, Battaglia VS (2012) Cooperation between active material, polymeric binder and conductive carbon additive in lithium ion battery cathode. *J Phys Chem C* 116:4875–4881
34. Zhu J, Lu L, Zeng KY (2013) Nanoscale mapping of lithium-ion diffusion in a cathode within an all-solid-state lithium-ion battery by advanced scanning probe microscopy techniques. *ACS Nano* 7:1666–1675
35. Zhu SM, Zhou HS, Miyoshi T, Hibino M, Honma I, Ichihara M (2004) Self-assembly of the mesoporous electrode material  $\text{Li}_3\text{Fe}_2(\text{PO}_4)_3$  using a cationic surfactant as the template. *Adv Mater* 16:2012–2017